JOURNAL OF BACTERIOLOGY, Aug. 2000, p. 4165–4172 Vol. 182, No. 15
0021-9193/00/$04.00+0

Characterization of a Second *tfd* Gene Cluster for Chlorophenol and Chlorocatechol Metabolism on Plasmid pJP4 in *Ralstonia eutropha* JMP134(pJP4)

CAROLINE M. LAEMMLI, JOHAN H. J. LEVEAU,† ALEXANDER J. B. ZEHNDER, AND JAN ROELOF VAN DER MEER*

Swiss Federal Institute for Environmental Science and Technology and Swiss Federal Institute for Technology, CH-8600 Dübendorf, Switzerland

Received 6 March 2000/Accepted 5 May 2000

Within the 5.9-kb DNA region between the *tfdR* and *tfdK* genes on the 2,4-dichlorophenoxyacetic acid (2,4-D) catabolic plasmid pJP4 from *Ralstonia eutropha* JMP134, we identified five open reading frames (ORFs) with significant homology to the genes for chlorocatechol and chlorophenol metabolism (*tfdCDEF* and *tfdB*) already present elsewhere on pJP4. The five ORFs were organized and assigned as follows: $tfdD_{II}C_{II}E_{II}F_{II}$ and $tfdB_{II}$ (in short, the tfd_{II} cluster), by analogy to *tfdCDEF* and *tfdB* (the tfd_{I} cluster). Primer extension analysis of mRNA isolated from 2,4-D-grown *R. eutropha* JMP134 identified a single transcription start site in front of the first gene of the cluster, $tfdD_{II}$, suggesting an operon-like organization for the tfd_{II} genes. By expressing each ORF in *Escherichia coli*, we confirmed that $tfdD_{II}$ coded for a chloromuconate cycloisomerase, $tfdC_{II}$ coded for a chlorocatechol 1,2-dioxygenase, $tfdE_{II}$ coded for a dienelactone hydrolase, $tfdF_{II}$ coded for a maleylacetate reductase, and $tfdB_{II}$ coded for a chlorophenol hydroxylase. Dot blot hybridizations of mRNA isolated from *R. eutropha* JMP134 showed that both tfd_{I} and tfd_{II} genes are transcribed upon induction with 2,4-D. Thus, the functions encoded by the tfd_{II} genes seem to be redundant with respect to those of the tfd_{I} cluster. One reason why the tfd_{II} genes do not disappear from plasmid pJP4 might be the necessity for keeping the regulatory genes for the 2,4-D pathway expression *tfdR* and *tfdS*.

Ralstonia eutropha JMP134(pJP4) was originally isolated in Australia from an unspecified soil sample by selection for its ability to use 2,4-dichlorophenoxyacetic acid (2,4-D) as sole carbon and energy source (6). The genes necessary for the metabolism of 2,4-D are located on a 22-kb DNA fragment of plasmid pJP4 (6) (Fig. 1). Among these, *tfdA* (33), *tfdB*, and *tfdCDEF* (8, 29) were the first genes to be identified. TfdA catalyzes the conversion of 2,4-D to 2,4-dichlorophenol (2,4-DCP) (13, 14), and TfdB catalyzes the conversion of 2,4-DCP to 3,5-dichlorocatechol (3,5-DCC) (12). The TfdCDEF enzymes catalyze the transformation of 3,5-DCC via 2,4-dichloromuconate (2,4-DCM) to 3-oxoadipate (12). Expression of the *tfd* pathway genes is regulated by the two identical LysR-type regulatory proteins, TfdR and TfdS (18, 19, 24, 27, 37). TfdT was long suspected to be a regulatory protein of the pathway as well, but it is actually a nonfunctional regulatory due to a C-terminal deletion caused by insertion of the insertion sequence (IS) element ISJP4 (24).

Plasmids for 2,4-D degradation such as pJP4 form a paradigm for the evolution of new catabolic pathways. The current hypothesis is that existing sets of genes from different organisms can be assembled into new structures, processes often catalyzed by mobile DNA elements (15). Indeed, mobile DNA elements associated with 2,4-D degradative genes are found in a number of plasmids such as pIJB1 and pJP4 (6, 36). In the case of plasmid pJP4, the IS element ISJP4 is thought to have been responsible for inserting a larger gene cassette containing (among others) the genes *tfdR* and *tfdS* (Fig. 1). Preliminary evidence had been obtained that another set of genes for chlorocatechol degradation might be present within this transposable element (17, 27), which was just recently confirmed (28), although this second cluster had not been previously detected by transposon mutagenesis studies (8). In addition, one novel function (*tfdK*) was discovered recently within this region (25). Located adjacent to ISPJ4, *tfdK* codes for an active transporter of 2,4-D at low-millimolar concentrations. This demonstrated that the 2,4-D pathway of *R. eutropha* JMP134 was even more complex than expected until then.

Here, we report the identification of a set of five genes in the 5.9-kb *tfdR-tfdK* intergenic region on plasmid pJP4. We provide evidence that this gene cluster, tfd_{II}, is actively transcribed in its host *R. eutropha* JMP134 and that it encodes the enzymes for the complete conversion of 2,4-DCP to β-ketoadipate. Although similar in structure and function, tfd_{II} is not simply a duplication of the *tfdCDEF-tfdB* (in short, tfd_{I}) gene cluster. Its role in 2,4-D degradation is subtle, redundant, and imperative as well, all of which seems to be the consequence of the past insertion of the ISJP4-flanked mobile element.

MATERIALS AND METHODS

Bacterial strains and growth conditions. *R. eutropha* JMP134(pJP4) is able to use 2,4-D and 3-chlorobenzoate as sole carbon and energy source (6, 7). *Escherichia coli* DH5α (30) was used for routine cloning purposes. *E. coli* BL21(DE3)(pLysS) (34), which carries the T7 RNA polymerase gene under control of the *lacUV5* promoter, was used for the T7-directed expression of pRSET6a-derived plasmids (31). *E. coli* cultures were grown in Luria-Bertani (LB) medium supplemented with ampicillin (100 μg/ml). *R. eutropha* cultures were grown in nutrient broth (Biolife, Milan, Italy) or in *Pseudomonas* mineral medium (16) supplemented with 10 mM fructose. Induction experiments were carried out with *R. eutropha* JMP134(pJP4) cultivated in a 1.5-liter chemostat on 10 mM fructose at a dilution rate of 0.05 h^{-1}. Induction of the 2,4-D pathway was achieved by addition of 2,4-D to the chemostat to a final concentration of 0.1 mM (23).

DNA manipulations, PCR, and sequence analysis. Plasmid DNA isolations, transformations, and other DNA manipulations were carried out according to

* Corresponding author. Mailing address: EAWAG, Überlandstrasse 133, P.O. Box 611, CH-8600 Dübendorf, Switzerland. Phone: 41 1 8235438. Fax: 41 1 8235547. E-mail: vdmeer@eawag.ch.

† Present address: Lindow Lab, Department of Plant and Microbial Biology, University of California, Berkeley, CA 94720-3102.

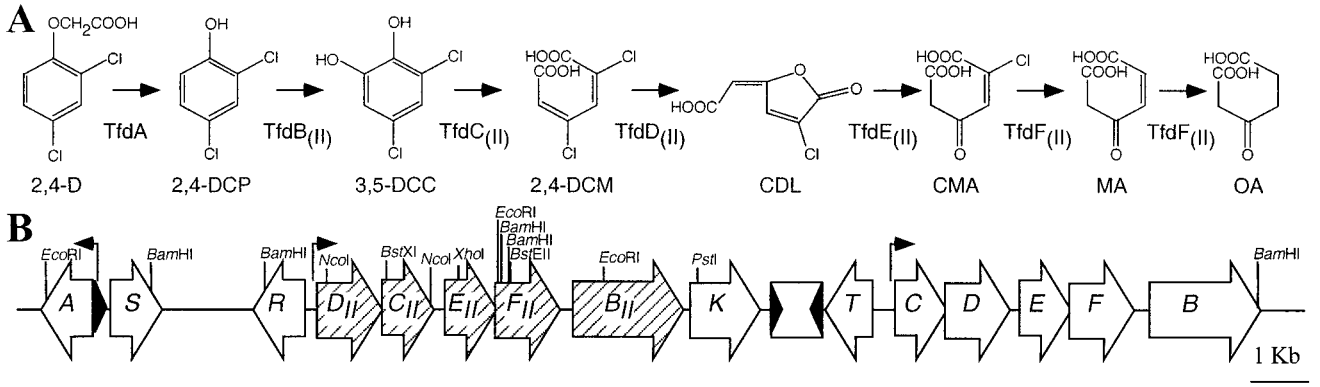

FIG. 1. (A) Overview of the steps in 2,4-D degradation. Enzymes catalyzing the different conversion steps: TfdA, 2,4-D α-ketoglutarate dioxygenase; $TfdB_{(II)}$, chlorophenol hydroxylase; $TfdC_{(II)}$, chlorocatechol 1,2-dioxygenase; $TfdD_{(II)}$, chloromuconate cycloisomerase; $TfdE_{(II)}$, dienelactone hydrolase; $TfdF_{(II)}$, (chloro)maleylacetate reductase. (B) Organization of the *tfd* genes on plasmid pJP4. Arrows indicate the sizes and orientations of all *tfd* genes currently known. The solid line represents noncoding DNA regions of pJP4. The rectangle between *tfdK* and *tfdT* represents the IS element ISJP4; black triangles depict the inverted repeats (not to scale). Positions of promoters regulated by TfdR(S) are indicated above the gene structure. All sites of the restriction enzymes *Bam*HI and *Eco*RI are indicated. Not all positions of the other depicted restriction enzymes are given. Abbreviations not given in the text: CDL, *cis*-DL; CMA, chloromaleylacetate; MA, maleylacetate; OA, 3-oxoadipate.

established procedures (30). Restriction enzymes and other DNA-modifying enzymes were obtained from Amersham Pharmacia Life Science (Cleveland, Ohio) or GIBCO/BRL Life Technologies Inc. (Gaithersburg, Md.) and used as specified by the manufacturer. Oligonucleotides for the PCR were obtained from Microsynth GmbH (Balgach, Switzerland). PCR mixtures contained 200 pmol of each primer per ml, 20 mM Tris-HCl (pH 8.4), 50 mM KCl, 0.05% (vol/vol) W-1, 2 mM $MgCl_2$, 0.25 mM each deoxynucleotide, and 30 U of *Taq* DNA polymerase (Life Technologies). DNA sequencing was performed on double-stranded DNA templates with a Thermo Sequenase cycle sequencing kit with 7-deaza-dGTP (Amersham). For sequencing of the tfd_{II} gene cluster, suitable overlapping subclones were generated for use as templates in sequencing reactions. Primers for sequencing were labeled with fluorescent dye IRD-800 or IRD-700 at the 5′ end and were purchased from MWG Biotech (Ebersberg, Germany). Fragments were separated on an automated DNA sequencer (model 4200 IR^2; LI-COR Inc., Lincoln, Neb.). Sequence assembly and computer analysis of the DNA sequences were done with the DNASTAR software (DNASTAR Inc., Madison, Wis.).

RNA isolation and primer extension analysis. RNA was isolated from chemostat-grown cultures of *R. eutropha* JMP134(pJP4), either under uninduced conditions (10 mM fructose) or induced with 0.1 mM 2,4-D, as described previously (2). DNase I-treated RNA samples were spotted on Hybond N+ membranes (Amersham) and hybridized with biotin-labeled antisense RNAs for each of the tfd_{II} open reading frames (ORFs) as described elsewhere (23). Primer extension reactions were carried out as follows. One microgram of total RNA from induced *R. eutropha* was annealed with 1 pmol of IRD800-labeled primer (for $tfdD_{II}$, 5′ CACGCTGCTCTGATGCTTGG 3′) in annealing buffer (Amersham) in a total volume of 5 μl. This amount was covered with one drop of mineral oil (Sigma), heated for 5 min at 68°C, and then cooled to 42°C. The reverse transcription reaction was started by addition of 3 μl of a mix containing avian myeloblastosis virus reaction buffer (Amersham), 6 U of avian myeloblastosis virus reverse transcriptase (Amersham), and 1.6 mM each deoxynucleotide. Reverse transcription reaction mixtures were incubated for 1 h at 42°C, then heated for 3 min at 95.5°C, and cooled on ice immediately. Samples of 1 μl from the reverse transcriptase reaction were mixed with 0.5 μl of formamide loading buffer and loaded onto a denaturing sequencing gel as described above. DNA sequencing reactions were prepared with the same IRD-labeled primer on double-stranded plasmid DNAs with the corresponding cloned pJP4 regions. Regions tested for cDNA synthesis on total RNA from induced *R. eutropha* cultures included $tfdD_{II}$, $tfdC_{II}$, $tfdB_{II}$, *tfdK*, and *tfdC*.

Plasmids. Plasmid pUC28 (3) was used as general cloning vector. pRSET6a (31) is a plasmid with a pBluescript (Stratagene, La Jolla, Calif.) backbone containing the specific expression elements of the pET3 vectors (34) and a newly designed multiple cloning site to facilitate cloning.

Translational fusions of each of the genes of the tfd_{II} cluster individually were constructed by fusing the ATG triplet of the *Nde*I site located in the multiple cloning site downstream of the T7 promoter and ribosome binding site on pRSET6a to the start codon of the respective *tfd* gene. DNA fragments containing either the $tfdC_{II}$, $tfdD_{II}$, or $tfdE_{II}$ ORF were custom-amplified by PCR, thereby introducing an *Nde*I site at the start codon and a *Bam*HI site downstream of the stop codon of each gene. The obtained PCR fragments were first cloned into the *Nde*I/*Bam*HI site of pUC28 and sequenced to confirm their identity with the original nucleotide sequence. The fragments were then reisolated and cloned into pRSET6a cut with *Nde*I and *Bam*HI. This resulted in plasmids pCBA199 ($tfdC_{II}$), pCBA165 ($tfdD_{II}$), pCBA202 ($tfdE_{II}$). Note that the $tfaD_{II}$ ORF starts at the ATG codon at position 1610 (numbering according to U16782).

For cloning the $tfdF_{II}$ gene, first a 240-bp fragment was amplified by PCR from plasmid pCBA83IV. The PCR-derived fragment was digested with *Nde*I and *Bam*HI and directly cloned to pRSET6a. A plasmid with the proper insert determined by sequencing was named pCBA179. To complete the ORF of $tfdF_{II}$, a 1.3-kb *Eco*RI fragment of pCBA88 was cloned into the *Eco*RI site of pCBA179 to give rise to plasmid pCBA184. The $tfdB_{II}$ gene was cloned as follows. First, a 620-bp fragment was amplified from plasmid pCBA84IV, using primers 981203 (5′ CGA TAA GGA GAC CAT ATG AACG 3′; $tfdB_{II}$ sequence) and 931011 (5′ TGA GCG GAT AAC AAT TT 3′; pUC18 sequence), digested with *Nde*I-*Eco*RI, and ligated into pUC28 cut with the same enzymes. After transformation, this resulted in plasmid pCBA174. The insert of pCBA174 was sequenced to confirm its identity. In a three-point ligation, the *Nde*I-*Eco*RI fragment of pCBA174 and the *Eco*RI-*Pst*I fragment of pCBA90 were ligated to pRSET6atfdD (U. Schell, Department of Microbiology, University of Stuttgart) cut with *Nde*I and *Pst*I to give pCBA180 (Table 1).

We then prepared frameshift mutations in each of the ORFs of the individually cloned tfd_{II} genes. For this purpose, plasmids pCBA199 ($tfdC_{II}$), pCBA165 ($tfdD_{II}$), pCBA202 ($tfdE_{II}$), pCBA184 ($tfdF_{II}$), and pCBA180 ($tfdB_{II}$) were each digested with a unique restriction site located in the respective tfd_{II} gene, treated with Klenow DNA polymerase, and religated (Table 1). By analogy, the truncated genes were named $tfdC_{II}\Delta$, $tfdD_{II}\Delta$, $tfdE_{II}\Delta$, $tfdF_{II}\Delta$, and $tfdB_{II}\Delta$, and the corresponding plasmids are pCBA200, pCBA196, pCBA201, pCBA197, and pCBA198 (Table 1).

Expression in *E. coli*. *E. coli* BL21(DE3)(pLysS) strains harboring pRSET6a-derived plasmids were grown in 50 ml of LB at 37°C to an optical density at 546 nm of between 0.5 and 0.6. To achieve induction, isopropyl-β-D-thiogalactopyranoside (IPTG) was added to the medium at a final concentration of 0.4 mM, and strains were incubated at 30°C for an additional 2.5 h. Cells were then centrifuged for 15 min at 5,300 rpm (4°C), washed with 20 ml of washing buffer (containing 20 mM Tris-HCl [pH 7.5] supplemented with 1 mM $MnSO_4$ in the case of *E. coli* expressing $tfdD_{II}$), and resuspended in 1 ml of washing buffer. Samples of 50 μl were taken from these cell suspensions for analysis by sodium dodecyl sulfate-polyacrylamide gel electrophoresis (SDS-PAGE), which was performed by the method of Laemmli (22). Disruption of the remainder of the cell suspensions was performed by sonication (Branson Sonifier 450; SCAN AG, Basel, Switzerland). One-milliliter cell suspensions were sonicated (five pulses of 15 s each) on ice at an output of 30 to 40 W, with a 1-min pause between pulses. Subsequently, suspensions were centrifuged at 4°C for 30 min at 15,000 × *g*. The resulting supernatants, referred to as cell extracts, were used in enzyme assays. Protein concentrations in the cell extracts were determined as described by Bradford (5), using bovine serum albumin as a standard.

Enzyme assays. All enzyme assays were performed by spectrophotometric methods in 0.5-ml quartz cuvettes at room temperature. Extinction coefficients were taken from Dorn and Knackmuss (9).

Chlorocatechol 1,2-dioxygenase activity was measured by determining product formation at 260 nm. Substrates tested included 3,5-DCC ($\varepsilon_{2,4\text{-DCM}}$ = 12,000 M^{-1} cm^{-1}), 3-chlorocatechol (3-CC) ($\varepsilon_{2\text{-CM}}$ = 17,100 M^{-1} cm^{-1}), or 4-CC ($\varepsilon_{3\text{-CM}}$ = 12,400 M^{-1} cm^{-1}). Reaction mixtures contained 40 mM Tris-HCl (pH 7.5), 0.3 mM EDTA, and 0.1 mM substrate. The reaction was started by adding cell extract (0.01 to 0.2 mg of protein).

Chloromuconate cycloisomerase activity was measured by determining the

TABLE 1. Plasmids constructed in this work

Plasmid	Description
pCBA83IV	pGEM-5Zf carrying the 870-bp *Nco*I-*Bam*HI fragment of pJP4 containing $tfdE_{II}$; Ap^r
pCBA84IV	pUC19 carrying the 1.3-kb *Bam*HI-*Eco*RI fragment of pJP4 containing part of $tfdF_{II}$ and $tfdB_{II}$; Ap^r
pCBA89	6.9-kb *Sac*I fragment of pJP4 in pUC
pCBA90	pUC19 carrying the 1.4-kb *Eco*RI-*Pst*I fragment of pJP4 containing part of $tfdB_{II}$ and *tfdK*; Ap^r
pCBA122	1-kb *Sac*II fragment of pCBA89; contains $tfdC_{II}$
pCBA174	pUC28 carrying a 550-bp *Nde*I-*Eco*RI fragment amplified by PCR from pCBA84IV; contains part of $tfdB_{II}$, Ap^r
pCBA179	pRSET6a carrying a 100-bp *Nde*I-*Bam*HI fragment amplified by PCR from pCBA83IV; contains part of $tfdF_{II}$; Ap^r
pCBA165	pRSET6a carrying the 1.2-kb *Nde*I-*Bam*HI fragment amplified from pCBA89; contains $tfdD_{II}$; Ap^r
pCBA180	pRSET6a carrying fragment *Nde*I-*Eco*RI from pCBA174 and fragment *Eco*RI-*Pst*I from pCBA90; contains complete $tfdB_{II}$; Ap^r
pCBA184	pCBA179 with the 1.3-kb *Eco*RI fragment from pCBA88; contains $tfdF_{II}$; Ap^r
pCBA192	pUC28 carrying a 800-bp *Nde*I-*Bam*HI fragment amplified from pCBA122; contains $tfdC_{II}$; Ap^r
pCBA196	pCBA165 with deletion of the *Nco*I site; contains frameshift mutation in $tfdD_{II}$; Ap^r
pCBA197	pCBA184 with deletion of the *Bst*EII site; contains frameshift mutation in $tfdF_{II}$; Ap^r
pCBA198	pCBA180 with deletion of the *Eco*RI site; contains frameshift mutation in $tfdB_{II}$; Ap^r
pCBA199	pRSET6a carrying the 800 bp *Nde*I-*Bam*HI fragment of pCBA192; contains $tfdC_{II}$; Ap^r
pCBA200	pCBA199 with deletion of the *Bst*XI site; contains frameshift mutation in $tfdC_{II}$; Ap^r
pCBA201	pCBA202 with deletion of the *Xho*I site; contains frameshift mutation in $tfdE_{II}$; Ap^r
pCBA202	pRSET6a carrying a 700-bp *Nde*I-*Bam*HI fragment amplified from pCBA89; contains $tfdE_{II}$; Ap^r

disappearance rate of substrate at 260 nm. Substrates used were 2-chloromuconate (2-CM), 3-CM, or freshly made 2,4-DCM (see below). Reaction mixtures contained 30 mM Tris-HCl (pH 7.5), 1 mM $MnSO_4$, and 0.1 mM substrate. Cycloisomerization of chloromuconates was assayed in the presence of an excess of dienelactone hydrolase to avoid accumulation of 4-carboxymethylene-but-2-en-4-olides. For the conversion of 2,4-DCM, an extinction coefficient of 5,800 M^{-1} cm^{-1} was used (21). The reaction was started by adding cell extract (0.01 to 0.2 mg of protein).

Dienelactone hydrolase activity was measured at 280 nm by determining the disappearance rate of substrate (*cis*-dienelactone [DL] [ε_{DL} = 17,000 M^{-1} cm^{-1}] or *trans*-DL). Reaction mixtures contained 10 mM histidine-HCl (pH 6.5) and 0.1 mM substrate. The reaction was started by adding cell extract (0.01 to 0.2 mg of protein).

Maleylacetate reductase activity was measured by determining maleylacetate-dependent NADH oxidation at 340 nm. Reaction mixtures contained 50 mM Tris-HCl (pH 7), 0.4 mM NADH, and cell extract (0.01 to 0.2 mg of protein). After the unspecific oxidation rate of NADH (ε_{NADH} = 6,300 M^{-1} cm^{-1}) was determined, the reaction was started by adding 0.4 mM freshly prepared maleylacetate (see below).

2,4-DCP dioxygenase was measured by determining 2,4-DCP-dependent NADPH oxidation at 340 nm. Reaction mixtures contained 60 mM phosphate buffer (pH 7.6), 0.03 mM flavin adenine dinucleotide, 0.3 mM NADPH, and cell extract (0.01 to 0.2 mg of protein). After the unspecific oxidation rate of NADPH (ε_{NADPH} = 6,300 M^{-1} cm^{-1}) was determined, the reaction was started by adding 0.05 mM 2,4-DCP.

Chemicals. 3-CC was a kind gift of Barbara Jakobs, GFB, Braunschweig, Germany. 4-CC and 3,5-DCC were purchased from Promochem GmbH (Wesel, Germany). 3-CM, *cis*-DL, and *trans*-DL were a kind gift from Walter Reineke, Bergische Universität-Gesamthochschule Wuppertal, Wuppertal, Germany. 2,4-DCM was prepared by incubation of a solution of 1 mM 3,5-DCC in 30 mM Tris-HCl (pH 8) with cell extract of *E. coli* BL21(pCBA199) expressing $tfdC_{II}$. The formation of 2,4-DCM was followed spectrophotometrically at 260 nm. After 20 min, the reaction mixture was centrifuged through a Centricon-10 (Amicon, Inc., Beverly, Mass.) filter at 5,000 × *g*. Maleylacetate was prepared by alkaline hydrolysis of *cis*-DL, as described elsewhere (11), by mixing 1 ml of 5 mM *cis*-DL with 7.5 μl of 2 N NaOH and incubating for 15 min at room temperature. 2,4-DCP was purchased from Fluka Chemie AG (Buchs, Switzerland).

Digital imaging. Sequence images were exported as TIFF files. Autoradiographic films and protein gels were scanned on a laser densitometer (Molecular Dynamics, Sunnyvale, Calif.) and exported as TIFF files. All TIFF files were imported into Adobe Photoshop (version 4.0; Adobe Systems, Inc., Mountain View, Calif.), cropped to the appropriate size, enhanced whenever necessary for reproduction, saved as gray scale TIFF files, and placed into Adobe Illustrator (version 8.0) for text additions.

Nucleotide sequence accession number. The sequence of the tfd_{II} gene cluster was deposited in GenBank under accession number U16782.

RESULTS

Identification of a second gene cluster for chlorophenol and chlorocatechol metabolism on pJP4. In the *tfdR-tfdK* intergenic region of plasmid pJP4, we located five ORFs with significant homology to genes for the metabolism of chlorinated phenols and catechols. The ORFs were arranged serially and in an orientation opposite that of the *tfdR* gene (Fig. 1). To signify their resemblance to genes from the *tfdCDEFB* cluster on pJP4, the ORFs were sequentially labeled $tfdD_{II}$, $tfdC_{II}$, $tfdE_{II}$, $tfdF_{II}$, and $tfdB_{II}$. The percentages of amino acid identity between the predicted polypeptides from the tfd_{II} genes and their counterparts from the *tfdCDEFB* genes varied substantially (Table 2). For example, $TfdE_{II}$ had only 15% predicted identical amino acids with TfdE, whereas $TfdC_{II}$ and TfdC shared 60% amino acid identity. The evolutionary relationships of the Tfd_{II} and Tfd_I gene products with other related proteins have been clearly pointed out elsewhere (10). These sequence comparisons indicated quite well that the tfd_{II} genes were not simply a duplication of the tfd_I cluster, or vice versa, but had a different evolutionary origin.

This became evident also from a comparison of the gene organization of the two clusters. In the tfd_{II} cluster, the $tfdD_{II}$ ORF preceded that of $tfdC_{II}$, whereas the opposite was found in the tfd_I cluster. Furthermore, no ORFs overlapped in the tfd_I cluster, whereas two cases of translational coupling (i.e., *tfdCD* and *tfdEF*) occur in the tfd_I cluster. In addition, the remainder of an ORF with unknown function exists between *tfdD* and *tfdE* which is similar to the *tcbCDEF* and *clcABDE* clusters but was absent in the tfd_{II} cluster. The tfd_{II} cluster showed highest percentages of identity to a set of *tfd* genes on plasmid pEST4011 of *Pseudomonas putida* and of *Variovorax paradoxus* (T. Valleys, L. Shengao, and K. Miyashita, unpublished data [DDBJ/EMBL/GenBank accession no. AB028643]). although smaller deletions or frameshift mutations must have occurred there. For example, the first 131 bp of the $tfdD_{II}$ ORF had 74% sequence identity to a region upstream of the *tfdC* gene of pEST4011, but no complete *tfdD* ORF exists. $TfdC_{II}$ had only 60% identical amino acids with TfdC, whereas it showed 83.5% identity with TfdC of pEST4011 (26). $TfdE_{II}$ carried 79.6% identical amino acid residues with the predicted polypeptide encoded by *tfdE* from *V. paradoxus*. Interestingly, the TfdE polypeptide predicted from *tfdE* on pEST4011 (26) had no significant similarity with $TfdE_{II}$ except for the first 22 amino acids, although the DNA sequence identity along the total 708-bp region in common was 77.4%. However, introducing a 2-bp frameshift into the *tfdE* ORF 66 bp downstream of the ATG start codon on pEST4011 would again result in a theoretical polypeptide with 79.6% similarity to $TfdE_{II}$ and 100% identity to TfdE of *V. paradoxus*.

TABLE 2. Features of the ORFs of the tfd_{I} and tfd_{II} gene clusters

ORF	Ribosome binding site	bp between RBS and start codon	Start codon	Location on sequence[a]	Length of ORF (bp)	Predicted molecular mass (kDa)	Pairwise identity (%)[b]
tfdC	GGAGG	4	GTG	337–1104	765	28.3	
$tfdC_{II}$	GAAGAG	8	ATG	2856–3617	759	28.1	60
tfdD	GGGGG	7	GTG	1101–2213	1,110	39.7	
$tfdD_{II}$[c]	−/GAAGCG	−/9	ATG/GTG	1610/1694–2659	1,047/963	36.9	35
tfdE	GGAG	7	ATG	2288–2992	702	25.4	
$tfdE_{II}$	GAAGG	7	ATG	3639–4346	705	25.4	15
tfdF	GAAGG	7	ATG	2989–4053	1,062	37.9	
$tfdF_{II}$	GGGGG	5	GTG	4348–5427	1,077	37.5	45
tfdB	GGAGG	5	ATG	4398–6194	1,794	65.4	
$tfdB_{II}$	GGAG	5	ATG	5495–7255	1,758	64.4	62

[a] GenBank accession no. M35097 (*tfdCDEFB*) and U16782 (tfd_{II} cluster).
[b] Calculated at the amino acid level.
[c] The slash indicates that there is no ribosome binding site corresponding to the ATG codon.

Finally, $TfdB_{II}$ carried 90.8% amino acid identity to TfdB of pEST4011.

Codon usage among genes of the tfd_{II} genes differed slightly from that of tfd_{I}: the two lysine codons TTA and TCT, the two serine codons TCT and AGT, and the two stop codons TAG and TAA did not occur in any of the tfd_{II} genes, whereas all possible codons occurred at least once in the tfd_{I} genes (Fig. 2B). This difference in codon usage may have effects on relative translation efficiency of the tfd_{II} or tfd_{I} mRNAs, for example, when codon demand does not coincide with specific tRNA abundance in the cell (35). Both clusters tended to use the codons containing a G or C wobble base more abundantly than those with A or T (Fig. 2B). This bias was reflected in the high average G+C content of both gene clusters; for *tfdCDEFB*, however, the G+C content was remarkably lower (56%) than that for the tfd_{II} cluster (66%) (Fig. 2A).

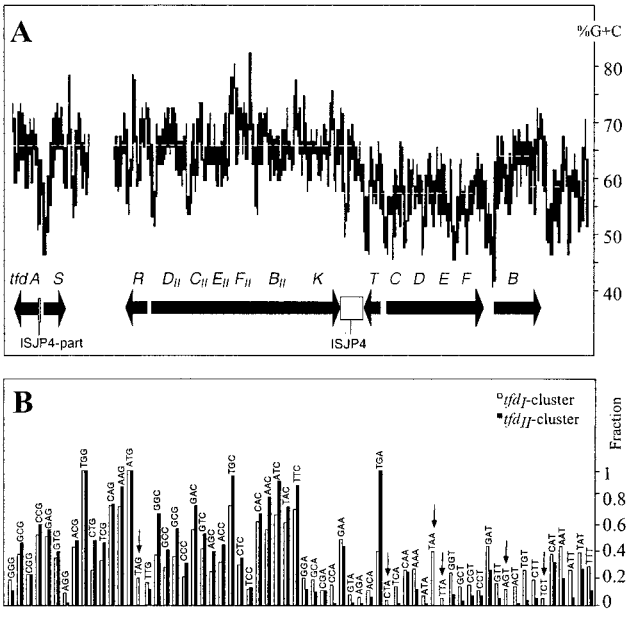

FIG. 2. (A) G+C content of the *tfd* region on plasmid pJP4. The graph was created using the program Curve.It (ICGEB, Trieste, Italy) with a window of 100 bp. Dotted lines indicate the average G+C content for distinct fragments. (B) Codon usage of the tfd_{I} and tfd_{II} gene clusters. The black and white bars represent the fraction of usage of a certain codon among all possible codons for a certain amino acid. Addition of all fractions of all possible codons for a certain amino acid gives a total fraction of 1. The codons are ordered by G+C content and wobble base, rich G+C content (left) to poor G+C content (right).

Expression of each of the tfd_{II} genes in *E. coli*. Cell extracts of *E. coli* BL21 cultures overexpressing each tfd_{II} gene individually were analyzed by SDS-PAGE (Fig. 3) and assayed for enzyme activities from the chlorocatechol and chlorophenol oxidative pathway (Table 3). As negative controls, induced cultures of each of the *E. coli* strains containing the plasmids with mutated tfd_{II} ORFs were used, along with *E. coli* BL21 without any pRSET plasmid. In total cell extract of *E. coli* BL21(pCBA165) expressing the $tfdD_{II}$ gene from its ATG start, we detected an overproduced polypeptide of about 42 kDa (Fig. 3, lane 5) which was absent in extracts of *E. coli* BL21(pCBA196) harboring a frameshift mutation in $tfdD_{II}$ (Fig. 3, lane 4). Chloromuconate cycloisomerase activity with 2,4-DCM and 3-CM as substrates was indeed detected in cell extracts of *E. coli* cultures harboring pCBA165 (Table 3). Significantly lower values were obtained when 2-CM was used as substrate. In cell extracts from cultures expressing the $tfdD_{II}$ frameshift mutant, however, no activity was found. Chlorocatechol 1,2-dioxygenase activity was clearly present in cell extracts from cultures expressing the $tfdC_{II}$ gene, with either 3,5-DCC, 3-CC, or 4-CC as substrate (Table 3). The predicted molecular mass of the polypeptide encoded by this ORF (28.1 kDa) fit well with the 27-kDa protein band determined by SDS-PAGE (Fig. 3, lane 2). No activity was detected in extracts of *E. coli* BL21 harboring the truncated gene $tfdC_{II}\Delta$. The observed peptide of 27 kDa in cell extracts of *E. coli* expressing $tfdC_{II}\Delta$ is caused by the frameshift at the *Bst*XI site, accidentally resulting in a peptide of the same size as $TfdC_{II}$.

With *cis*- and *trans*-DL as substrates, dienelactone hydrolase activity was clearly detected in cell extracts from cultures expressing $tfdE_{II}$. This activity coincided with the production of a 25-kDa protein (Fig. 3, lane 8). In contrast, we found no such polypeptide (Fig. 3, lane 7) and also no hydrolase activity with cells expressing $tfdE_{II}\Delta$ from plasmid pCBA201. Maleylacetate reductase activity was detected in cell extracts of *E. coli* BL21 harboring $tfdF_{II}$ by monitoring the maleylacetate-dependent oxidation of NADH (Table 3). In these cell extracts, SDS-PAGE revealed a protein with an apparent mass of about 37 kDa, which is close to the theoretically predicted mass of 37.5 kDa (Fig. 3, lane 10). This protein band was absent in total cell extracts of *E. coli* BL21(pCBA197), carrying a frameshift mutation in $tfdF_{II}$ (Fig. 3, lane 9). Both *E. coli* BL21(pCBA184) and *E. coli* (pCBA197) strongly produced a 27-kDa protein, which might be the result of a translational fusion protein starting at nucleotide position 3844 (numbering according to

TABLE 3. Enzyme specific activities encoded by the tfd_{II} genes measured in cell extracts of *E. coli* BL21

Gene	Plasmid	Sp act (mU/mg of protein)[a]									
		CC 1,2-D[b]			CMC			DLH		MAR, MA	2,4-DPH, 2,4-DCP
		3,5-DCC	3-CC	4-CC	2,4-DCM	2-CM	3-CM	*cis*-DL	*trans*-DL		
$tfdC_{II}$	pCBA199	10^3	0.8×10^3	0.6×10^3		—			—	—	—
$tfdC_{II}\Delta$[c]	pCBA200	2	4	2		—			—	—	—
$tfdD_{II}$	pCBA165		—[d]		4.4×10^3	60	2×10^3		—	—	—
$tfdD_{II}\Delta$	pCBA196		—		−3	−1	6		—	—	—
$tfdE_{II}$	pCBA202		—			—		2.6×10^3	2×10^3	—	—
$tfdE_{II}\Delta$	pCBA201		—			—		17	4	—	—
$tfdF_{II}$	pCBA184		—			—			—	3.6×10^3	—
$tfdF_{II}\Delta$	pCBA197		—			—			—	37	—
$tfdB_{II}$	pCBA180		—			—			—	—	7
$tfdB_{II}\Delta$	pCBA198		—			—			—	—	2
None		—	1.1	—	—	—	1.7	1.1	—	31	—

[a] 1 U = 1 μmol of substrate disappearance or product formation per min. Shown are representative values from one activity assay. Assays were performed at least in independent triplicates.

[b] CC 1,2-D, chlorocatechol 1,2-dioxygenase; CMC, chloromuconate cycloisomerase; DLH, dienelactone hydrolase; MAR, maleylacetate reductase; 2,4-DPH, 2,4-dichlorophenol hydroxylase; DCC, dichlorocatechol; CC, chlorocatechol; DCM, dichloromuconate; CM, chloromuconate; DL, dienelactone; MA, maleylacetate; DCP, dichlorophenol

[c] Frameshift in $tfdC_{II}$.

[d] —, not measured.

GenBank entry U16782) and continuing in pRSET6a. A slight background activity was found with cell extracts expressing a frameshift mutated $tfdF_{II}$ and in cell extracts from *E. coli* without any pRSET-type plasmid (Table 3). We suppose, therefore, that this low activity is due to native proteins from *E. coli* itself. Finally, the activity of $TfdB_{II}$ was determined in cell extracts of *E. coli* BL21 harboring $tfdB_{II}$ and compared to that in cell extracts of *E. coli* BL21 containing the frameshift mutated $tfdB_{II}\Delta$. The activities measured for $TfdB_{II}$ were lower than those of the other Tfd_{II} enzymes but still higher than the activities measured in the negative control. The molecular mass of the $TfdB_{II}$ protein in cells harboring pCBA180 was as predicted (65 kDa) (Fig. 3, lane 13). In *E. coli*(pCBA198) containing a frameshift mutation in the $tfdB_{II}$ gene, we observed a protein of 24 kDa, which is the size of the generated truncated $TfdB_{II}\Delta$ protein (Fig. 3, lane 12). Based on these results, we conclude that the Tfd_{II} enzymes catalyzed the transformations expected from their similarities to the Tfd_I counterparts.

Expression of the tfd_{II} genes in *R. eutropha* JMP134(pJP4). Since enzyme assays in extracts from *R. eutropha* JMP134 do not allow us to distinguish between activities from the tfd_I cluster and the corresponding ones from the tfd_{II} cluster, we relied on specific mRNA analysis to determine if transcription from the tfd_{II} genes occurred. Induction of transcription was shown by hybridizing total RNA, isolated from a continuous culture at different time points after addition of 0.1 mM 2,4-D to the medium, with probes for the different tfd_{II} genes. Immediately after addition of 2,4-D, levels of mRNA of the $tfdC_{II}$ gene increased rapidly, followed shortly by those of $tfdE_{II}$, $tfdB_{II}$, and *tfdK* (Fig. 4). Maximum levels of mRNA were reached 14 min after induction, after which there was a de-

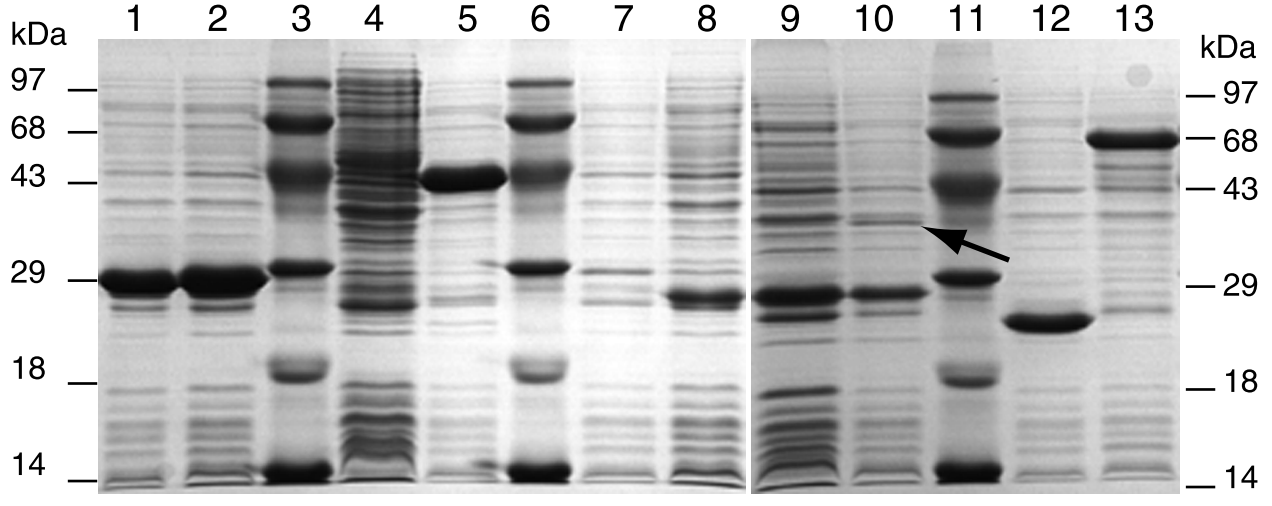

FIG. 3. SDS-polyacrylamide gel of total cell extracts of IPTG-induced *E. coli* BL21(DE3)(pLysS) strains harboring pRSET6a-derived plasmids carrying one of the tfd_{II} genes or its truncated derivative. Lanes: 1, pCBA200 ($tfdC_{II}\Delta$); 2, pCBA199 ($tfdC_{II}$); 3, molecular size marker; 4, pCBA196 ($tfdD_{II}\Delta$); 5, pCBA165 ($tfdD_{II}$); 6, molecular size marker; 7, pCBA201 ($tfdE_{II}\Delta$); 8, pCBA202 ($tfdE_{II}$); 9, pCBA197 ($tfdF_{II}\Delta$); 10, pCBA184 ($tfdF_{II}$); 11, molecular size marker; 12, pCBA198 ($tfdB_{II}\Delta$); 13, pCBA180 ($tfdB_{II}$). Positions of molecular masses are indicated on the left and right. The arrow in lane 10 points to the putative $TfdF_{II}$ protein. (Digital image was recorded as a TIFF file; background was enhanced for reproduction in Adobe Photoshop.)

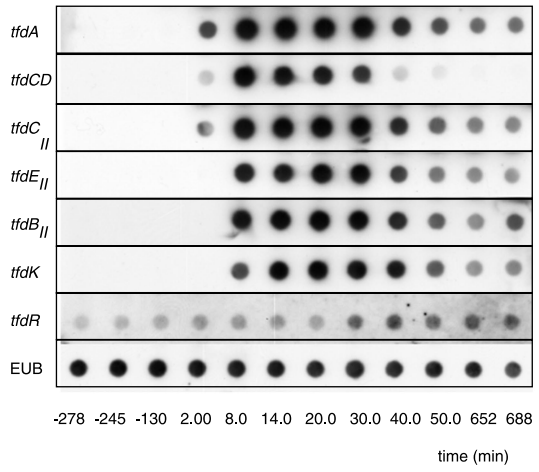

FIG. 4. Dot blot hybridizations of total RNA isolated from a chemostat-grown culture of *R. eutropha* JMP134 before and after induction with 2,4-D. Antisense RNA probes are indicated on the left. Times at which the samples were taken from the chemostat are indicated at the bottom. 2,4-D was introduced into the chemostat at time zero. Panels for each hybridization were obtained in independent hybridization experiments; therefore, signal intensities cannot be directly compared between different probes. In addition, spot densities were not corrected for small differences among total RNA amounts spotted at each position. Note the distinct and immediate strong induction for all markers except *tfdR* and EUB (=16S rRNA). (Digital image was obtained by scanning of original autoradiograms; individual TIFF files were compiled in Adobe Photoshop.)

crease in mRNA to a stable level that remained unchanged for over 10 h. We observed a similar pattern of gene induction for the *tfdA* and *tfdCD* genes (Fig. 4). Expression of *tfdR*, as well as that of the gene for 16S rRNA, remained essentially unchanged upon addition of 2,4-D (Fig. 4).

To map transcriptional start sites of the tfd_{II} gene cluster, we performed primer extension analysis on total RNA that was isolated from chemostat-grown cells of *R. eutropha* JMP134(pJP4) under uninduced and induced (i.e., with 2,4-D) conditions. Using a primer positioned in the $tfdD_{II}$ gene, we were able to detect a specific cDNA transcript which was not observed from an uninduced culture (Fig. 5). The product identified a single transcription start site at a G residue at position −82 relative to the putative GTG or +3 relative to the postulated ATG translation start codon of $tfdD_{II}$ (Fig. 5). This makes the GTG a more likely candidate for the translation start codon of the $tfdD_{II}$ gene (Fig. 5). We found no primer extension products from primers positioned in the reading frames of any of the other genes of the tfd_{II} cluster, including *tfdK*. These results suggest an operon-like organization for the genes $tfdD_{II}$ to *tfdK*. From the location of the transcriptional start site, we propose a TTAGAC/TAGACT promoter sequence for $tfdD_{II}$ (Fig. 5). Control primer extension reactions with a primer complementary to *tfdC* resulted in transcription starts at T and G (nucleotides 286 and 287), 4 nucleotides downstream of the −10 region proposed by Perkins (29) (not shown).

DISCUSSION

Further exploration of the ISJP4-flanked transposable element on pJP4 led us to discover five ORFs, potentially encoding the metabolism of chlorocatechols and of chlorophenols. The ORFs were designated $tfdD_{II}$, $tfdC_{II}$, $tfdE_{II}$, $tfdF_{II}$, and $tfdB_{II}$, by analogy to the *tfdCDEFB* genes on pJP4. We demonstrated by expressing each individual ORF in *E. coli* that the ORF designated $tfdD_{II}$ codes for a chloromuconate cycloisomerase, $tfdC_{II}$ codes for a chlorocatechol 1,2-dioxygenase, $tfdE_{II}$ codes for a dienelactone hydrolase, $tfdF_{II}$ codes for a maleylacetate reductase, and $tfdB_{II}$ codes for a chlorophenol hydroxylase. Together with the previously characterized *tfd* genes, this brings to eight the number of genes that are presently included in the transposable DNA: *tfdS*, *tfdR*, and $tfdD_{II}C_{II}E_{II}F_{II}B_{II}K$. Substantial evidence leads us to believe that the tfd_{I} and tfd_{II} genes were acquired from different origins rather than evolved by duplication and divergence within one host. First, the actual percentages of identity among counterparts in the tfd_{I} and tfd_{II} clusters were rather low (15 to 62% at the amino acid level). Second, the G+C content of the tfd_{II} genes

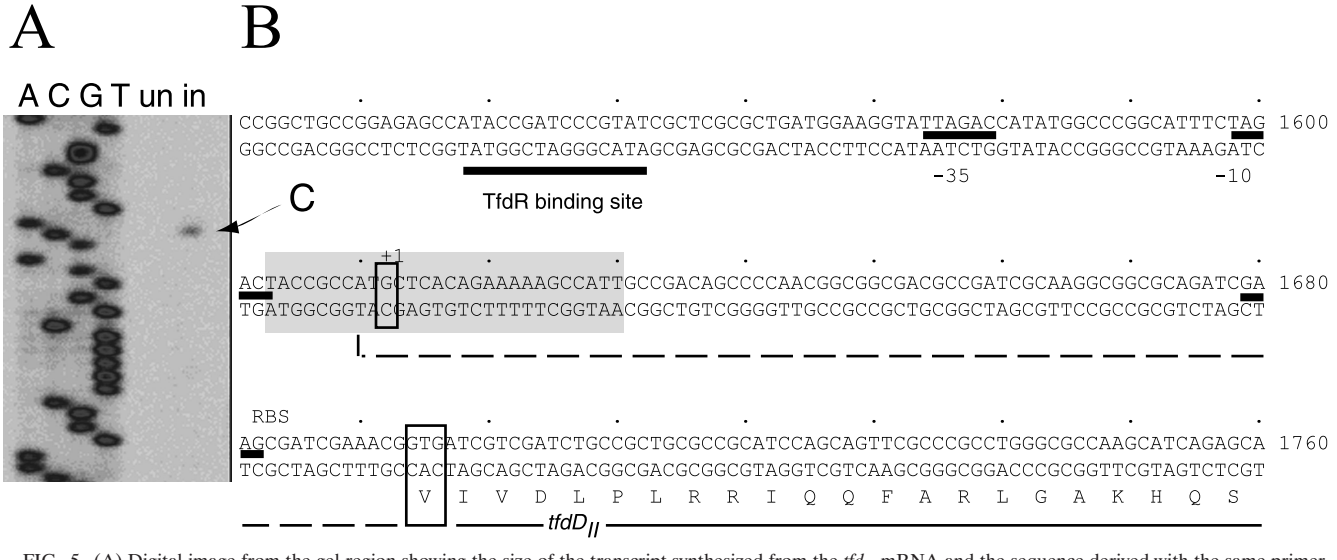

FIG. 5. (A) Digital image from the gel region showing the size of the transcript synthesized from the tfd_{II} mRNA and the sequence derived with the same primer. (Image recorded as a TIFF file on a LI-COR IR^2 sequencer; background enhanced for reproduction purposes in Adobe Photoshop). The arrow points to the specific transcript observed under induced (in; with 2,4-D) conditions. un, uninduced. (B) Relevant part of the DNA sequence upstream of the $tfdD_{II}$ ORF. Translation of $tfdD_{II}$ is shown from the second possible start (Val at position 1694). The dotted line represents continuation of the ORF in the upstream direction. The first start codon (ATG at position 1612), however, was identified as the position of the transcription start (indicated with +1). Possible promoter elements and the TfdR binding site are indicated. The shaded region represents the sequence showed in the digital image.

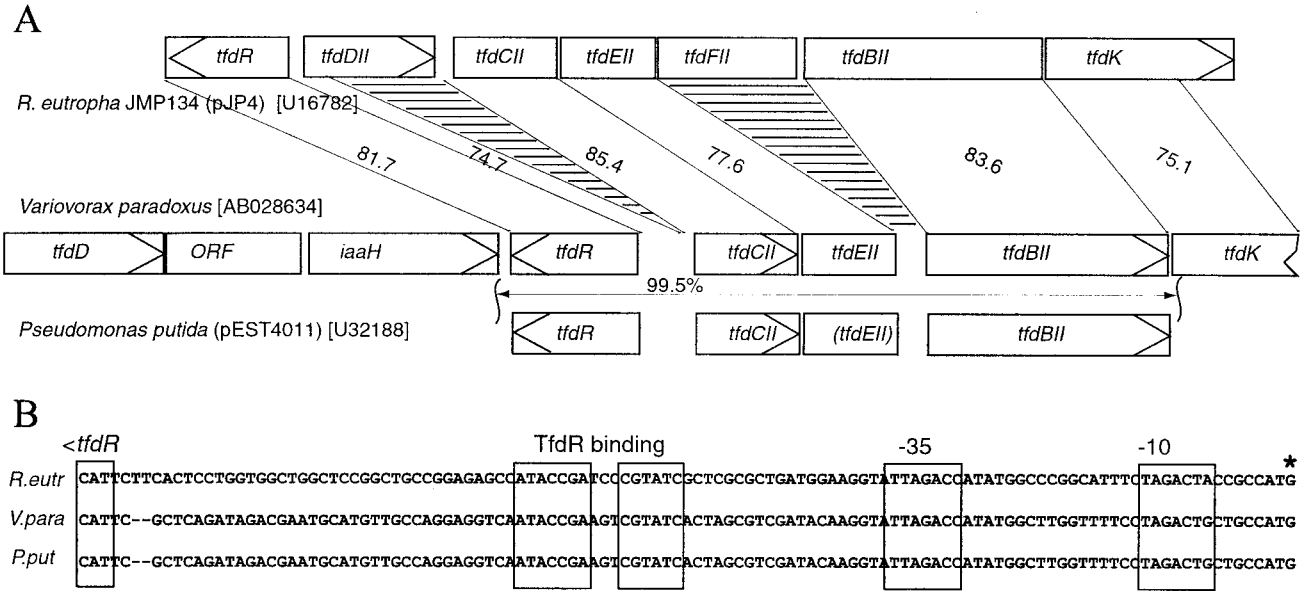

FIG. 6. (A) Comparison of the genetic organizations of the tfd_{II} clusters of *R. eutropha* JMP134, *V. paradoxus* (Valleys et al., unpublished), and *P. putida* (pEST4011) (20). Connecting lines point to regions of high sequence identity among the different gene clusters. Percentages of sequence identity are given between the gene maps. The striped areas indicate regions deleted from the tfd_{II} cluster of *R. eutropha* compared to the others. GenBank accession numbers are given in panel A. (B) Sequence alignment of the intergenic regions directly upstream of *tfdR* in the direction of $tfdD_{II}$ (for *R. eutropha*) or *tfdC* (for *V. paradoxus* and pEST4011). Boxed regions point to the conserved TfdR binding motif and to the −35 and −10 promoter sequences. The asterisk indicates the mapped transcription start site for the *R. eutropha* tfd_{II} operon.

is significantly higher (Fig. 2). Since *tfdS* and *tfdR* are fully identical, and perhaps themselves the result of a duplication event, we suppose that at one point a DNA fragment containing *tfdR* and $tfdD_{II}C_{II}E_{II}F_{II}B_{II}K_{II}$ flanked by ISJP4 was mobilized into an ancestor pJP4 plasmid.

The results obtained with expression in *E. coli* showed that the tfd_{II} genes can encode 2,4-DCP-metabolizing enzymes. Furthermore, we showed that the tfd_{II} genes are transcribed in *R. eutropha* when cells are exposed to 2,4-D. Although we could not directly demonstrate that the tfd_{II} genes are indeed translated into functional enzymes in *R. eutropha* JMP134, it seems rather unlikely that they would not be. First, all of the tfd_{II} genes are transcribed and induced upon exposure of the cells to 2,4-D, and as strongly as the genes from the cluster tfd_I (Fig. 5). Second, at least three gene products from the tfd_{II} cluster are synthesized during growth on 2,4-D: TfdR, the regulatory protein of all the pathway genes; TfdK, a transporter protein for 2,4-D; and $TfdF_{II}$, the maleylacetate reductase (19, 24, 25, 27, 32). Accidentally, the purified active enzyme catalyzing 2-chloromaleylacetate reduction in *R. eutropha* JMP134 turned out to be $TfdF_{II}$, which was proven by NH_2-terminal sequencing of the purified protein (32). Moreover, it was recently demonstrated that *R. eutropha* strains with a plasmid containing the tfd_{II} gene cluster could actually grow on 3-chlorobenzoate (28). This makes it unlikely that the tfd_{II} genes would not be translated in *R. eutropha* JMP134, although especially the $tfdD_{II}$ ORF has a very poor ribosome binding site. Strangely enough, the tfd_{II} genes were not detected along with the tfd_I genes in the original transposon mutagenesis studies performed by Don et al. (8). We can at least rule out that the tfd_{II} cluster was inserted on pJP4 after their analysis, since the physical map of plasmid pJP4 as drawn by Don and Pemberton in 1985 (6) is identical to the current map determined from DNA sequencing data.

At this point, the question arises as to why the present-day configuration of the *tfd* genes with two sets of homologous genes is kept on plasmid pJP4 as it is. One answer is that at least some of the functions encoded within the tfd_{II} cluster are favorable for growth on 2,4-D. Such a function might indeed be the chloromaleylacetate reductase $TfdF_{II}$. TfdF transposon mutants grew poorly on 2,4-D but well on 3-chlorobenzoate (8), which suggests that not TfdF but $TfdF_{II}$ actually catalyzes the dechlorination of 2-chloromaleylacetate during growth on 2,4-D. Another function specific for the tfd_{II} cluster is TfdK, a transporter protein which facilitates uptake of 2,4-D at low extracellular concentrations. However, TfdK does not seem to be indispensable for growth (25). A more important function, however, is carried by the regulatory protein TfdR (or its identical twin TfdS). Since TfdR is the transcriptional activator for *tfdA* expression and for both the tfd_I and the tfd_{II} genes (19, 24, 27), its loss would abolish 2,4-D pathway induction. Most likely, if the tfd_{II} cluster were to become lost from pJP4, this would occur through recombination of homologous regions or activity of the ISJP4 element. Recombination between the right-end partial copy of ISJP4 (located between *tfdS* and *tfdA*) and ISJP4 (downstream of *tfdK*) would lead to loss of the regulatory genes. An alternative, perhaps more seldom, recombination between *tfdT* and *tfdR* would lead to loss of the tfd_{II} cluster but could still restore the regulatory function. At least one plasmid with this type of recombination seems to exist, i.e., pMAB1. Restriction analysis of pMAB1 suggests identical *tfdCDEF* genes as on pJP4 but a recombination between *tfdT* and *tfdR* (21). This again points to the importance of maintaining proper regulation of the *tfd* pathway genes. Therefore, it seems that the current configuration is locked into a semistable state, due to the presence of the current regulatory genes within the tfd_{II} cluster and the inactivated original regulatory gene (*tfdT*) lying in the tfd_I cluster.

We can speculate a little on the genealogy of the tfd_{II} cluster, since at least two other genetic systems for 2,4-D degradation are known to carry *tfd*-type genes with higher identities to the tfd_{II} cluster of pJP4 than to the tfd_I cluster (Fig. 6). One of

these occurs on plasmid pEST4011, which is a derivative of a plasmid (pEST4002) originally isolated from *P. putida* strain EST4002 from 2,4-D-treated soils in Estonia (1). One region on this plasmid contains tfd_{II}-type genes, although in a configuration, *tfdR-tfdC-*(*tfdE*)*-tfdB*, without $tfdD_{II}$, $tfdF_{II}$, or *tfdK* (20). Regulatable expression of chlorocatechol 1,2-dioxygenase and chlorophenol hydroxylase activities was demonstrated for this region of plasmid pEST4011 (26). The other system from *V. paradoxus* is basically identical to the *tfd* genes of pEST4011, although more sequence information is available on regions upstream of *tfdR* and downstream of *tfdB* (Valleys et al., unpublished). This indicated that a *tfdK*-like gene was downstream of *tfdB* and a *tfdD*-like gene was further upstream of *tfdR* (Fig. 6). Interestingly, in at least one region (between *tfdR* and *tfdC*), a deletion has occurred which removed part of the $tfdD_{II}$ ORF on pEST4011, leaving only 131 bp of the $tfdD_{II}$ ORF and the intergenic region between *tfdR* and $tfdD_{II}$ (Fig. 6A). This part, however, might be still important for a proper regulation of *tfd* gene expression, since it carries the TfdR binding site (Fig. 6B). At least in the *V. paradoxus* system, a complete *tfdD* gene copy exists, which, however, has a higher percentage sequence identity to $tfdD_{I}$ (64.2) than to $tfdD_{II}$ (55.2). Between *tfdC* and *tfdB* is a 708-bp sequence with 77.4% identity with $tfdE_{II}$, but a frameshift hinders the production of a $TfdE_{II}$-like polypeptide. This frameshift is not present in the *V. paradoxus* sequence. Curiously, no traces of the $tfdF_{II}$ gene can be found in the *V. paradoxus* or pEST4011 sequence. This finding suggests that this region of pEST4011 and of *V. paradoxus* was derived from a tfd_{II}-like cluster and points to a wider distribution of the tfd_{II}-type cluster among soil microorganisms rather than a single occurrence on pJP4.

ACKNOWLEDGMENT

The work of C.M.L. was supported by grant 31-49222.96 from the Swiss National Science Foundation.

REFERENCES

1. **Ausmees, N. R., and A. L. Heinaru.** 1990. New plasmids of herbicide 2,4-dichlorophenoxyacetic acid biodegradation. Genetika **26:**770–772.
2. **Baumann, B., M. Snozzi, A. J. Zehnder, and J. R. van der Meer.** 1996. Dynamics of denitrification activity of *Paracoccus denitrificans* in continuous culture during aerobic-anaerobic changes. J. Bacteriol. **178:**4367–4374.
3. **Benes, V., Z. Hostomsky, L. Arnold, and V. Paces.** 1993. M13 and pUC vectors with new unique restriction sites for cloning. Gene **130:**151–152.
4. **Bhat, M. A., M. Tsuda, K. Horiike, M. Nozaki, C. S. Vaidyanathan, and T. Nakazawa.** 1994. Identification and characterization of a new plasmid carrying genes for degradation of 2,4-dichlorophenoxyacetate from *Pseudomonas cepacia* CSV90. Appl. Environ. Microbiol. **60:**307–312.
5. **Bradford, M. M.** 1976. A rapid and sensitive method for the determination of microgram quantities of protein utilizing the principle of protein-dye binding. Anal. Biochem. **72:**248–254.
6. **Don, R. H., and J. M. Pemberton.** 1985. Genetic and physical map of the 2,4-dichlorophenoxyacetic acid degradative plasmid pJP4. J. Bacteriol. **161:** 466–468.
7. **Don, R. H., and J. M. Pemberton.** 1981. Properties of six pesticide degradation plasmids isolated from *Alcaligenes paradoxus* and *Alcaligenes eutrophus*. J. Bacteriol. **145:**681–686.
8. **Don, R. H., A. J. Weightman, H. J. Knackmuss, and K. N. Timmis.** 1985. Transposon mutagenesis and cloning analysis of the pathways for degradation of 2,4-dichlorophenoxyacetic acid and 3-chlorobenzoate in *Alcaligenes eutrophus* JMP134 (pJP4). J. Bacteriol. **161:**85–90.
9. **Dorn, E., and H. J. Knackmuss.** 1978. Chemical structure and biodegradability of halogenated aromatic compounds. Substituent effects on 1,2-dioxygenation of catechol. Biochem. J. **174:**85–94.
10. **Eulberg, D., E. M. Kourbatova, L. A. Golovleva, and M. Schlömann.** 1998. Evolutionary relationship between chlorocatechol catabolic enzymes from *Rhodococcus opacus* 1CP and their counterparts in proteobacteria: sequence divergence and functional convergence. J. Bacteriol. **180:**1082–1094.
11. **Evans, W. C., B. S. W. Smith, H. N. Fernley, and J. I. Davies.** 1971. Bacterial metabolism of 2,4-dichlorophenoxyacetate. Biochem. J. **122:**543–551.
12. **Farhana, L., and P. B. New.** 1997. The 2,4-dichlorophenol hydroxylase of *Alcaligenes eutrophus* JMP134 is a homotetramer. Can. J. Microbiol. **43:**202–205.
13. **Fukumori, F., and R. P. Hausinger.** 1993. *Alcaligenes eutrophus* JMP134 "2,4-dichlorophenoxyacetate monooxygenase" is an alpha-ketoglutarate-dependent dioxygenase. J. Bacteriol. **175:**2083–2086.
14. **Fukumori, F., and R. P. Hausinger.** 1993. Purification and characterization of 2,4-dichlorophenoxyacetate/alpha-ketoglutarate dioxygenase. J. Biol. Chem. **268:**24311–24317.
15. **Fulthorpe, R. R., C. McGowan, O. V. Maltseva, W. E. Holben, and J. M. Tiedje.** 1995. 2,4-Dichlorophenoxyacetic acid-degrading bacteria contain mosaics of catabolic genes. Appl. Environ. Microbiol. **61:**3274–3281.
16. **Gerhardt, P., R. G. E. Murray, R. N. Costilow, E. W. Nester, W. A. Wood, N. R. Krieg, and G. B. Phillips.** 1981. Manual of methods for general bacteriology. American Society for Microbiology, Washington, D.C.
17. **Ghosal, D., and I.-S. You.** 1988. Nucleotide homology and organization of chlorocatechol oxidation genes of plasmids pJP4 and pAC27. Mol. Gen. Genet. **211:**113–120.
18. **Harker, A. R., R. H. Olsen, and R. J. Seidler.** 1989. Phenoxyacetic acid degradation by the 2,4-dichlorophenoxyacetic acid (TFD) pathway of plasmid pJP4: mapping and characterization of the TFD regulatory gene, *tfdR*. J. Bacteriol. **171:**314–320.
19. **Kaphammer, B., J. J. Kukor, and R. H. Olsen.** 1990. Regulation of *tfdCDEF* by *tfdR* of the 2,4-dichlorophenoxyacetic acid degradation plasmid pJP4. J. Bacteriol. **172:**2280–2286.
20. **Koiv, V., R. Marits, and A. Heinaru.** 1996. Sequence analysis of the 2,4 dichlorophenol hydroxylase gene *tfdB* and 3,5 dichlorocatechol 1,2 dioxygenase gene *tfdC* of 2,4 dichlorophenoxyacetic acid degrading plasmid pEST4011. Gene **174:**293–297.
21. **Kuhm, A. E., M. Schlömann, H.-J. Knackmuss, and D. H. Pieper.** 1990. Purification and characterization of dichloromuconate cycloisomerase from *Alcaligenes eutrophus* JMP 134. Biochem. J. **266:**877–883.
22. **Laemmli, U. K.** 1970. Cleavage of structural proteins during the assembly of the head of bacteriophage T4. Nature **227:**680–685.
23. **Leveau, J. H. J., F. König, H. Füchslin, C. Werlen, and J. R. van der Meer.** 1999. Dynamics of multigene expression during catabolic adaptation of *Ralstonia eutropha* JMP134 (pJP4) to the herbicide 2,4-dichlorophenoxyacetate. Mol. Microbiol. **33:**396–406.
24. **Leveau, J. H. J., and J. R. van der Meer.** 1996. The *tfdR* gene product can successfully take over the role of the insertion element-inactivated TfdT protein as a transcriptional activator of the *tfdCDEF* gene cluster, which encodes chlorocatechol degradation in *Ralstonia eutropha* JMP134 (pJP4). J. Bacteriol. **178:**6824–6832.
25. **Leveau, J. H. J., A. J. B. Zehnder, and J. R. van der Meer.** 1997. The *tfdK* gene product facilitates the uptake of 2,4-dichlorophenoxyacetate by *Ralstonia eutropha* JMP134 (pJP4). J. Bacteriol. **180:**2237–2243.
26. **Maë, A. A., R. O. Marits, N. R. Ausmees, V. M. Kôiv, and A. L. Heinaru.** 1993. Characterization of a new 2,4-dichlorophenoxyacetic acid degrading plasmid pEST4011: physical map and localization of catabolic genes. J. Gen. Microbiol. **139:**3165–3160.
27. **Matrubutham, U., and A. R. Harker.** 1994. Analysis of duplicated gene sequences associated with *tfdR* and *tfdS* in *Alcaligenes eutrophus* JMP134. J. Bacteriol. **176:**2348–2353.
28. **Perez-Pantoja, D., L. Guzman, M. Manzano, D. H. Pieper, and B. Gonzalez.** 2000. Role of $tfdC_ID_IE_IF_I$ and $tfdD_{II}C_{II}E_{II}F_{II}$ gene modules in catabolism of 3-chlorobenzoate by *Ralstonia eutropha* JMP134(pJP4). Appl. Environ. Microbiol. **66:**1602–1608.
29. **Perkins, E. J., M. P. Gordon, O. Caceres, and P. F. Lurquin.** 1990. Organization and sequence analysis of the 2,4-dichlorophenol hydroxylase and dichlorocatechol oxidative operons of plasmid pJP4. J. Bacteriol. **172:**2351–2359.
30. **Sambrook, J., E. F. Fritsch, and T. Maniatis.** 1989. Molecular cloning: a laboratory manual. Cold Spring Harbor Laboratory, Cold Spring Harbor, N.Y.
31. **Schoepfer, R.** 1993. The pRSET family of T7 promoter expression vectors for *Escherichia coli*. Gene **124:**83–85.
32. **Seibert, V., F. K. Stadler, and M. Schlömann.** 1993. Purification and characterization of maleylacetate reductase from *Alcaligenes eutrophus* JMP134 (pJP4). J. Bacteriol. **175:**6745–6754.
33. **Streber, W. R., K. N. Timmis, and M. H. Zenk.** 1987. Analysis, cloning, and high-level expression of 2,4-dichlorophenoxyacetate monooxygenase gene *tfdA* of *Alcaligenes eutrophus* JMP134. J. Bacteriol. **169:**2950–2955.
34. **Studier, F. W., and B. A. Moffatt.** 1986. Use of bacteriophage T7 RNA polymerase to direct selective high-level expression of cloned genes. J. Mol. Biol. **189:**113–130.
35. **Xia, X.** 1998. How optimized is the translational machinery in *Escherichia coli*, *Salmonella typhimurium* and *Saccharomyces cerevisiae*? Genetics **149:** 37–44.
36. **Xia, X. S., S. Aathithan, K. Oswiecimska, A. R. W. Smith, and I. J. Bruce.** 1998. A novel plasmid pIJB1 possessing a putative 2,4-dichlorophenoxyacetic acid degradative transposon Tn*5530* in *Burkholderia cepacia* strain 2a. Plasmid **39:**154–159.
37. **You, I. S., and D. Ghosal.** 1995. Genetic and molecular analysis of a regulatory region of the herbicide 2,4-dichlorophenoxyacetate catabolic plasmid pJP4. Mol. Microbiol. **16:**321–331.